

The determination of high energy particle spectra via gamma ray regularized inversion

Federico Benvenuto

Dipartimento di Matematica
Genova

benvenuto@dima.unige.it

July 29, 2016

15 RHESSI meeting Graz

Joint work with:

Gordon Emslie, Richard Schwartz,
Alec MacKinnon, Michele Piana, Gabriele Torre

A γ -ray spectrum

Share, Murphy, APS Conference Series

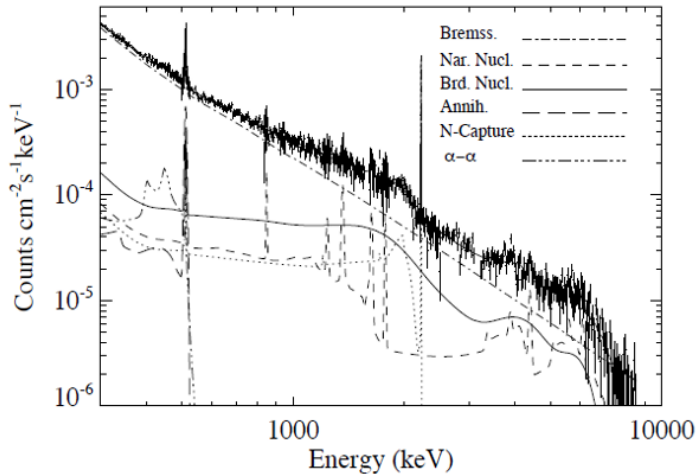


Figure: Count spectrum of the 2002 July 23 solar flare with fits revealing different components.

Ingredients for γ -ray solar flare spectra

Energy range : $100\text{KeV} - 8\text{MeV}$

Many different interactions and physical processes contributing to X -ray and γ -ray solar flare spectra.

- **electrons**

X -ray and γ -ray Bremsstrahlung

- **ions**

γ -ray line radiation (1-8 MeV) (narrow and broad lines)

$\alpha - \alpha$ -particle interaction

neutron capture line (2.223 MeV)s

Line radiation model

- L: number of ambient species
- K: number of accelerated species

$$I_{line}(\epsilon) \Delta\epsilon = \sum_{k=1}^K \sum_{\ell=1}^L a_\ell \int_0^\infty j_{k,\ell}(\epsilon, E) F_k(E) dE. \quad (1)$$

- $\{F_k(E)\}_{k=1}^K$ Accelerated ion spectra
- $j_{k,l}(\epsilon, E)$ Interaction integral kernel
- $I(\epsilon)\Delta\epsilon$ emergent γ -line spectrum
- a_ℓ Ambient abundances

Nuclear deexcitation gamma-ray lines from accelerated particle interactions,
ApJS, Kozlovsky Murphy Ramaty 2002

Interaction kernel

What does the interaction integral kernel contain ?

- 24 spectra for the narrow lines
- - accelerated H, 4He and 3He interacting with the eight ambient elements 4He, 24 12C, 14N, 16O, 20Ne, 24Mg, 28Si, 56Fe
- 14 spectra for the broad lines
- - accelerated 12C, 14N, 16O, 20Ne, 24Mg, 28Si, 56Fe interacting with ambient H and 4He

Discretized framework

- $x_p \sim (F_1(E), \dots, F_K(E))$
- $H_{i,\ell,p} \sim j_{k,\ell}(\epsilon, E) \quad (E, k) \rightarrow p \quad \epsilon \rightarrow i$

Let us consider the problem to find a , x and g once y is given and described by the equation:

Inverse Problem

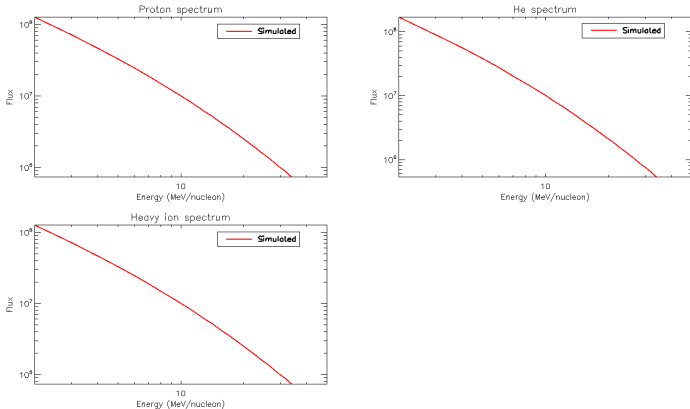
$$y_i = f(\textcolor{red}{a}, \textcolor{red}{x}) = \sum_{\ell=1}^L \textcolor{red}{a}_\ell \sum_{p=1}^{KM} H_{i,\ell,p} \textcolor{red}{x}_p + b_i$$

Take a look at the forward model

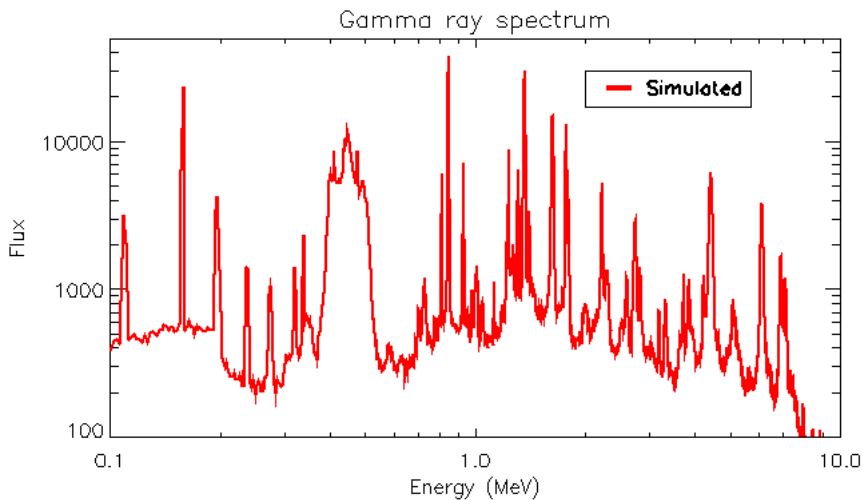
Ambient
abundances

H : 1.00E-00
HH : 1.00E-01
C : 2.96E-04
N : 7.90E-05
O : 6.37E-04
Ne : 9.55E-05
Mg : 1.25E-04
Al : 1.00E-05
Si : 9.68E-05
S : 2.03E-05
Ca : 6.75E-06
Fe : 8.54E-05

Input spectra: Bessel functions



Take a look at the forward model



Generated using the 'Murphy code'

Inverse Problem as optimization

Assumptions:

- the data y has to be realizations of a Poisson random variable.
- x , a and b have non-negative components;

The standard **Maximum Likelihood** approach boils down to find the solution x, a which minimizes the

C-statistic

$$C(x, y) = \frac{2}{N} \sum_{i=0}^N y_i \log \left(\frac{y}{aHx + b} \right)_i + (aHx + b)_i - y_i \quad (2)$$

Inverse methods

If you consider the abundances to be known = a , it is a linear problem:
a popular **non parametric** inversion method is the

Richardson Lucy

$$x_{k+1} = x_k \ P \star \frac{y}{P \star x_k}$$

where P is a point spread function, $P*$ and $P\star$ indicate convolution and correlation.

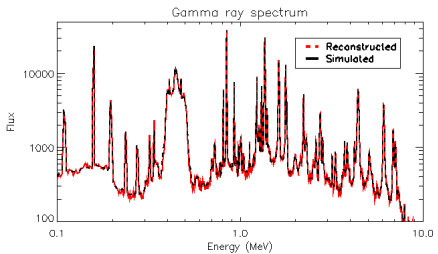
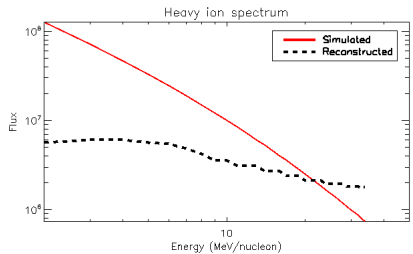
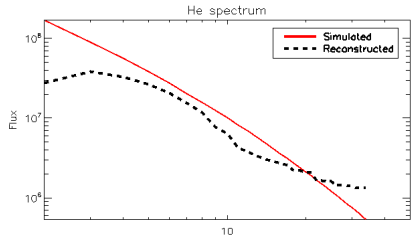
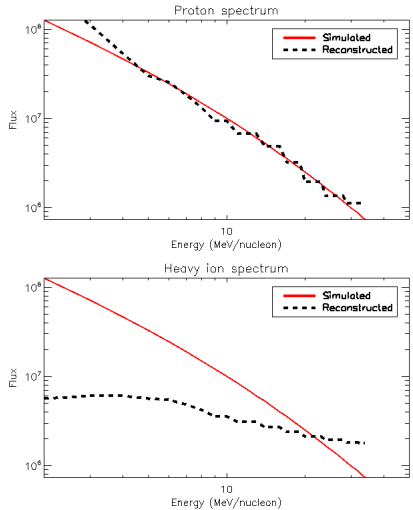
Here we use its generalization:

Expectation Maximization

$$x_{k+1} = \frac{x_k}{(aH)^T 1} (aH)^T \frac{y}{aHx_k}$$

where we have aH (k), row-column multiplication (convolution) and column-row multiplication (correlation).

Inversion with known abundances



Blind expectation-maximization

Take another step towards reality

$$y = f(a, x, z) = aHx + Qz + b$$

- background b unknown (+ Bremsstrahlung effect)
- ambient abundances a unknown

Inspired by the blind deconvolution scheme

INIT : set x_0 , z_0 and a_0

$$STEP\ 1 : \quad x_{k+1} = \frac{x_k}{(a_k H)^T 1} (a_k H)^T \frac{y}{a_k H x_k + Q z_k + b}$$

$$STEP\ 2 : \quad a_{k+1} = \frac{a_k}{(H x_{k+1})^T 1} (H x_{k+1})^T \frac{y}{a_k H x_{k+1} + Q z_k + b}$$

$$STEP\ 3 : \quad z_{k+1} = \frac{z_k}{Q^T 1} Q^T \frac{y}{a_{k+1} H x_{k+1} + Q z_k + b}$$

Repeat STEP 1,2 and 3 until a given condition is met (stop criterion)

Inversion method

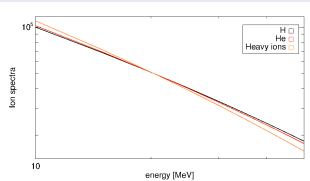
Some comments:

- The used method is convergent as shown in Lee & Seung, Neural Information Processing Systems (2000) to an optimized solution.
- From a numerical point of view the solution is unique, but the key point is the $\alpha - \alpha$ interaction.
- Perform several inversions (several initializations x_0, a_0, z_0) with fixed carbon ambient abundance. Select the optimal one.

Simulations

Input spectra for energetic ions:

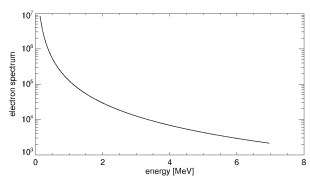
$$N(E) \simeq AK_2 \left[\left(\frac{E}{mc^2} \right)^{\frac{1}{4}} \right]$$



Ramaty R., Murphy R. J., *Nuclear processes and accelerated particles in solar flares*, 1987

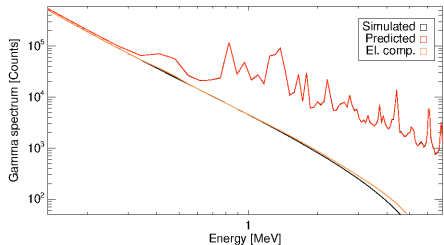
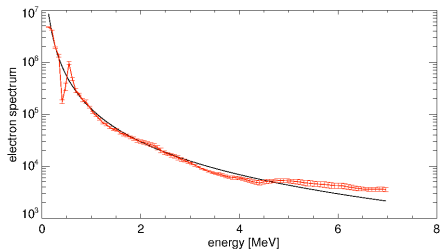
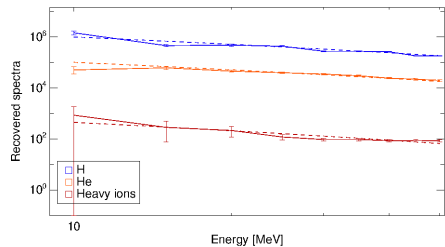
Input spectra for energetic electrons:

$$F(E) = B \left(\frac{E_0}{E} \right)^{2.9}$$



Share G., H. Murphy R. J., *Solar gamma-ray line spectroscopy - physics of a flaring star*, 2004

Simulation: high statistic



Black line under the red one represents simulated data (Fermi bins)

Simulation: high statistic

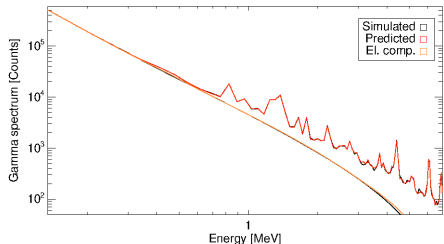
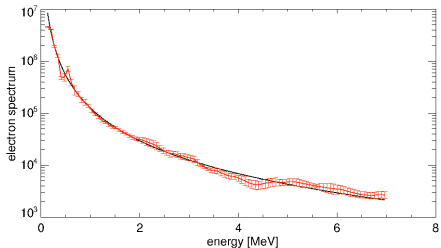
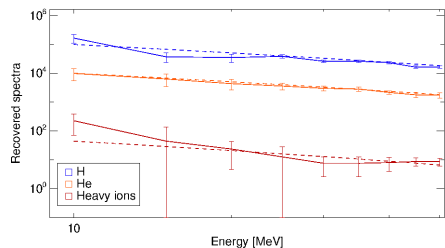
Ambient Abundances

| | | |
|----|----------------------------|----------------------|
| H | 1.0 ± 0.0 | 1.0 |
| He | 0.084 ± 0.005 | 0.1 |
| C | $(4.34 \pm 0.00)10^{-4}$ | $4.34 \cdot 10^{-4}$ |
| N | $(1.67 \pm 0.11)10^{-4}$ | $1.57 \cdot 10^{-4}$ |
| O | $(1.058 \pm 0.024)10^{-3}$ | 10^{-3} |
| Ne | $(4.11 \pm 0.12)10^{-4}$ | $4 \cdot 10^{-4}$ |
| Mg | $(4.20 \pm 0.08)10^{-4}$ | $4.08 \cdot 10^{-4}$ |
| Al | $(6.8 \pm 0.6)10^{-5}$ | $6.8 \cdot 10^{-5}$ |
| Si | $(3.68 \pm 0.07)10^{-4}$ | $3.52 \cdot 10^{-4}$ |
| S | $(1.205 \pm 0.022)10^{-4}$ | $1.17 \cdot 10^{-4}$ |
| Ca | $(9.21 \pm 0.25)10^{-5}$ | $8.8 \cdot 10^{-5}$ |
| Fe | $(1.116 \pm 0.022)10^{-3}$ | $1.08 \cdot 10^{-3}$ |

Energetic Abundances

| | | |
|----|--------------------------|----------------------|
| H | 1.00 ± 0.19 | 1.0 |
| He | 0.082 ± 0.018 | 0.1 |
| C | $(5.8 \pm 3.6)10^{-4}$ | $4.34 \cdot 10^{-4}$ |
| N | $(1.52 \pm 1.01)10^{-4}$ | $1.57 \cdot 10^{-4}$ |
| O | $(1.7 \pm 1.4)10^{-3}$ | 10^{-3} |
| Ne | $(2.8 \pm 0.9)10^{-4}$ | $4 \cdot 10^{-4}$ |
| Mg | $(4.9 \pm 2.7)10^{-4}$ | $4.08 \cdot 10^{-4}$ |
| Al | $(0.55 \pm 1.04)10^{-4}$ | $6.8 \cdot 10^{-5}$ |
| Si | $(3.59 \pm 2.09)10^{-4}$ | $3.52 \cdot 10^{-4}$ |
| S | $(1.31 \pm 1.09)10^{-4}$ | $1.17 \cdot 10^{-4}$ |
| Ca | $(2.81 \pm 3.07)10^{-4}$ | $8.8 \cdot 10^{-5}$ |
| Fe | $(8.6 \pm 2.4)10^{-4}$ | $1.08 \cdot 10^{-3}$ |

Simulation: medium statistic



Black line under the red one represents simulated data (Fermi bins)

Simulation: medium statistic

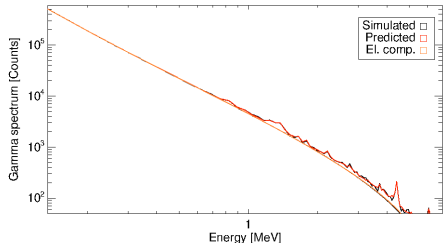
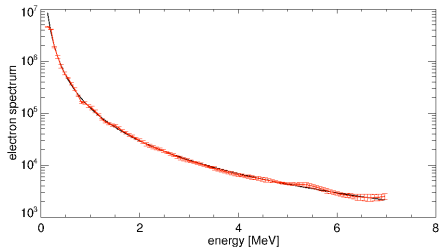
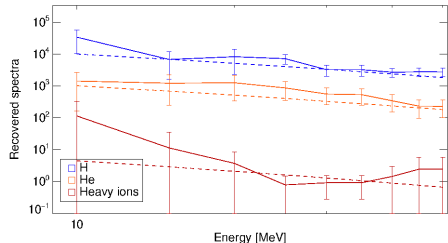
Ambient Abundances

| | | |
|----|--------------------------|-----------------------|
| H | 1.0 ± 0.0 | 1.0 |
| He | 0.02 ± 0.014 | 0.1 |
| C | $(4.34 \pm 0.0)10^{-4}$ | $4, 34 \cdot 10^{-4}$ |
| N | $(1.9 \pm 0.5)10^{-4}$ | $1.57 \cdot 10^{-4}$ |
| O | $(1.18 \pm 0.09)10^{-3}$ | 10^{-3} |
| Ne | $(4.4 \pm 0.5)10^{-4}$ | $4 \cdot 10^{-4}$ |
| Mg | $(4.6 \pm 0.3)10^{-4}$ | $4.08 \cdot 10^{-4}$ |
| Al | $(4.2 \pm 5.2)10^{-5}$ | $6.8 \cdot 10^{-5}$ |
| Si | $(4.2 \pm 0.3)10^{-4}$ | $3.52 \cdot 10^{-4}$ |
| S | $(1.29 \pm 0.11)10^{-4}$ | $1.17 \cdot 10^{-4}$ |
| Ca | $(9.89 \pm 1.05)10^{-5}$ | $8.8 \cdot 10^{-5}$ |
| Fe | $(1.22 \pm 0.09)10^{-3}$ | $1.08 \cdot 10^{-3}$ |

Energetic Abundances

| | | |
|----|--------------------------|----------------------|
| H | 1.0 ± 0.5 | 1.0 |
| He | 0.09 ± 0.06 | 0.1 |
| C | $(1.4 \pm 2.1)10^{-3}$ | $4.34 \cdot 10^{-4}$ |
| N | $(6.6 \pm 8.9)10^{-4}$ | $1.57 \cdot 10^{-4}$ |
| O | $(3.4 \pm 3.6)10^{-3}$ | 10^{-3} |
| Ne | $(2.9 \pm 2.9)10^{-4}$ | $4 \cdot 10^{-4}$ |
| Mg | $(0.79 \pm 1.02)10^{-3}$ | $4.08 \cdot 10^{-4}$ |
| Al | $(0.86 \pm 2.8)10^{-4}$ | $6.8 \cdot 10^{-5}$ |
| Si | $(4.9 \pm 9.9)10^{-4}$ | $3.52 \cdot 10^{-4}$ |
| S | $(0.61 \pm 1.12)10^{-4}$ | $1.17 \cdot 10^{-4}$ |
| Ca | $(5.3 \pm 7.4)10^{-4}$ | $8.8 \cdot 10^{-5}$ |
| Fe | $(1.32 \pm 1.16)10^{-3}$ | $1.08 \cdot 10^{-3}$ |

Simulation: low statistic



Black line under the red one represents simulated data (Fermi bins)

Simulation: low statistic

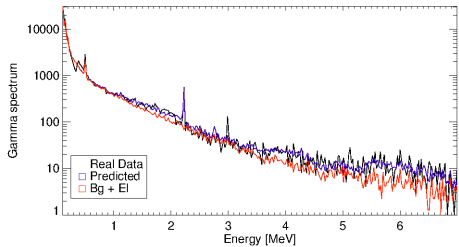
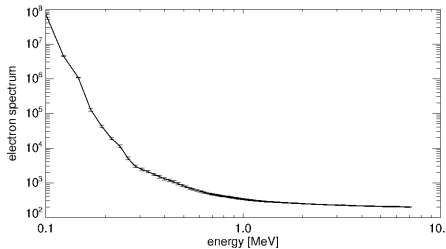
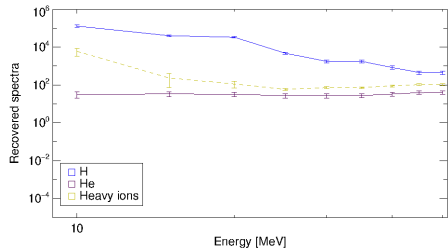
Ambient Abundances

| | | |
|----|-------------------------|----------------------|
| H | 1.0 ± 0.0 | 1.0 |
| He | $(3.0 \pm 5.2)10^{-7}$ | 0.1 |
| C | $(4.34 \pm 0.0)10^{-4}$ | $4.34 \cdot 10^{-4}$ |
| N | $(0.8 \pm 1.1)10^{-4}$ | $1.57 \cdot 10^{-4}$ |
| O | $(6.4 \pm 1.3)10^{-4}$ | 10^{-3} |
| Ne | $(3.2 \pm 0.8)10^{-4}$ | $4 \cdot 10^{-4}$ |
| Mg | $(3.0 \pm 0.5)10^{-4}$ | $4.08 \cdot 10^{-4}$ |
| Al | $(0.5 \pm 1.7)10^{-4}$ | $6.8 \cdot 10^{-5}$ |
| Si | $(2.6 \pm 0.9)10^{-4}$ | $3.52 \cdot 10^{-4}$ |
| S | $(8.9 \pm 2.6)10^{-5}$ | $1.17 \cdot 10^{-4}$ |
| Ca | $(5.6 \pm 2.2)10^{-5}$ | $8.8 \cdot 10^{-5}$ |
| Fe | $(6.5 \pm 1.2)10^{-5}$ | $1.08 \cdot 10^{-8}$ |

Energetic Abundances

| | | |
|----|------------------------|----------------------|
| H | 1.0 ± 1.2 | 1.0 |
| He | 0.09 ± 0.12 | 0.1 |
| C | $(0.7 \pm 1.7)10^{-3}$ | $4.34 \cdot 10^{-4}$ |
| N | $(1.5 \pm 2.5)10^{-4}$ | $1.57 \cdot 10^{-4}$ |
| O | $(2.2 \pm 5.3)10^{-3}$ | 10^{-3} |
| Ne | $(5.4 \pm 7.1)10^{-4}$ | $4 \cdot 10^{-4}$ |
| Mg | $(3.3 \pm 4.8)10^{-3}$ | $4.08 \cdot 10^{-4}$ |
| Al | $(0.6 \pm 1.5)10^{-2}$ | $6.8 \cdot 10^{-5}$ |
| Si | $(1.2 \pm 2.6)10^{-5}$ | $3.52 \cdot 10^{-4}$ |
| S | $(2.6 \pm 9.9)10^{-4}$ | $1.17 \cdot 10^{-4}$ |
| Ca | $(0.4 \pm 1.3)10^{-3}$ | $8.8 \cdot 10^{-5}$ |
| Fe | $(6.4 \pm 9.2)10^{-3}$ | $1.08 \cdot 10^{-3}$ |

28 November 2003 event



28 November 2003 event

Ambient Abundances

| | |
|----|--------------------------|
| H | 1.0 ± 0.0 |
| He | $(3.7 \pm 0.4)10^{-5}$ |
| C | $(2.2 \pm 2.5)10^{-4}$ |
| N | $(3.9 \pm 3.2)10^{-5}$ |
| O | $(1.8 \pm 2.4)10^{-4}$ |
| Ne | $(9.1 \pm 5.6)10^{-5}$ |
| Mg | $(3.28 \pm 1.19)10^{-4}$ |
| Al | $(3.1 \pm 4.9)10^{-5}$ |
| Si | $(4.9 \pm 1.7)10^{-4}$ |
| S | $(2.45 \pm 0.11)10^{-3}$ |
| Ca | $(5.5 \pm 6.4)10^{-5}$ |
| Fe | $(3.3 \pm 1.6)10^{-6}$ |

Energetic Abundances

| | |
|----|--------------------------|
| H | 1.00 ± 0.24 |
| He | $(1.4 \pm 0.5)10^{-3}$ |
| C | $(2.52 \pm 1.06)10^{-3}$ |
| N | $(3.90 \pm 1.15)10^{-3}$ |
| O | $(3.0 \pm 0.8)10^{-1}$ |
| Ne | $(4.04 \pm 1.09)10^{-3}$ |
| Mg | $(1.6 \pm 0.8)10^{-4}$ |
| Al | $(2.6 \pm 2.4)10^{-4}$ |
| Si | $(1.6 \pm 0.7)10^{-2}$ |
| S | $(3.30 \pm 1.06)10^{-3}$ |
| Ca | $(1.5 \pm 1.5)10^{-3}$ |
| Fe | $(9.2 \pm 3.3)10^{-4}$ |

To be continued

- A fundamental issue is the background subtraction
- RHESSI spectra have a high energy resolution
- Shift effect can make the fit procedure totally ineffective.

Possible solutions:

- Produce a family of models parametrized by the acceleration angle.
 - choose which model gives the best fit (if any)
- Introduce a parameter for each species for modeling the shift.
 - Is there an efficient optimization strategy for solving the inverse problem?
- Extract the main peaks of a RHESSI gamma ray spectrum and shift them at the 'right' energy (those of the Murphy code).
 - what to do with broader lines ?
- Convolve both the gamma ray data and the gamma ray model output by a psf in order to dump the doppler shift.
 - how large the psf should be ?